Integration of ferroelectric $Pb(Zr_{0.52}Ti_{0.48})O_3$ thin films on conducting nanocrystalline diamond for high performance device applications

Martando Rath, Dinesh Kumar, and M. S. Ramachandra Rao

Citation: Appl. Phys. Lett. **113**, 032904 (2018); doi: 10.1063/1.5035450
View online: https://doi.org/10.1063/1.5035450
View Table of Contents: http://aip.scitation.org/toc/apl/113/3
Published by the American Institute of Physics

Integration of ferroelectric $Pb(Zr_{0.52}Ti_{0.48})O_3$ thin films on conducting nanocrystalline diamond for high performance device applications

Martando Rath, Dinesh Kumar, and M. S. Ramachandra Rao[a)]
Department of Physics, Nano Functional Materials Technology Centre, Indian Institute of Technology Madras, Chennai 600036, India

(Received 16 April 2018; accepted 5 July 2018; published online 20 July 2018)

We report on the direct integration of a $Pb(Zr_{0.52}Ti_{0.48})O_3$ (PZT) thin film on a hot filament chemical vapor deposition grown conducting boron doped nanocrystalline diamond (B-NCD) film. A conducting B-NCD thin film with a grain size less than 100 nm and surface roughness close to 8 nm is used as a metallic bottom electrode. X-ray diffraction and Raman spectroscopy revealed the single phase perovskite ferroelectric nature of the pulsed laser deposited grown PZT thin film directly on the conducting B-NCD substrate with an electrical resistivity of 10 mΩ-cm. The PZT thin film grown on the B-NCD/Si substrate showed the high remanent polarization ($2P_r$) of 68 $\mu C/cm^2$ and high dielectric constant of ~1300 with a low leakage current density of $\sim 10^{-5}$ A/cm^2. Macroscopic and nanoscale polarization switching experiments are performed to confirm the ferroelectric nature of the PZT/B-NCD capacitor. A very small degradation of remanent polarization of 10% even after 10^{10} switching cycles of the sample demonstrates the excellent ferroelectric performance of the multilayer. *Published by AIP Publishing*. https://doi.org/10.1063/1.5035450

Modern day electronic industries demand fabrication of high performance devices such as micro/nano electromechanical systems (M/NEMS), non-volatile ferroelectric random access memory (NVFRAM), and surface acoustic wave (SAW) devices.[1–3] These require integration of ferroelectric/piezoelectric thin films with suitable substrates to enable the intrinsic properties and functionalities of the devices.[4] Among all the ferroelectric materials, $Pb(Zr_xTi_{1-x})O_3$ (PZT) is a potential candidate because of its excellent ferroelectric and piezoelectric properties.[5–7] PZT thin films have been grown on different substrates such as Si, $SrTiO_3$, YBCO, GaN, diamond, Ni, Cu, and Inconel[4,8–14] to understand the influence of substrates on their functional properties for intended applications.

Si is being widely used for device fabrication because it exhibits minimal mechanical hysteresis and high dimensional stability and possesses a low thermal expansion coefficient.[10,15] However, it may not be suitable for high frequency RF MEMS/NEMS resonators and switches because of its low Young's modulus (130 GPa) and hardness (1000 kg/mm^2).[16,17] In RF MEMS/NEMS devices, a piezoelectric material such as PZT is sandwiched between top and bottom electrodes and induces strain upon the application of potential difference across the piezoelectric materials.[16] For potential high frequency RF MEMS/NEMS applications, PZT should be integrated with a structural material having high Young's modulus with high hardness which can withstand for higher frequencies.[15,17] In the scenario where higher Young's modulus and hardness are required, chemical vapor deposited (CVD) diamond films with robust physical properties such as high thermal conductivity, high Young's modulus (=1200 GPa), and high operating frequencies would be more suitable materials to integrate with piezoelectric materials for radio frequency (RF) MEMS/NEMS devices.[1,16]

Direct integration of PZT on diamond is a challenging task because of the thermal mismatch that exists between them.[8] Considerable efforts have been put forward recently in realizing PZT on a diamond substrate.[10,15,17] Du *et al.* demonstrated that the formation of the pyrochlore phase leads to degradation of ferroelectric properties in the multilayer.[18] To avoid formation of the pyrochlore phase, Liao *et al.* used buffer layers such as Al_2O_3, Pt, and $SrTiO_3$ between the PZT thin film and the diamond substrate.[15,18] However, it was found that the PZT/diamond with buffer layers is undesirable because of interface diffusion issues and complexity in device fabrication. Therefore, direct integration of PZT on the diamond substrate is highly desirable and an ultimate necessity. Recently, our group has grown PZT on insulating diamond without using any buffer layers.[19] The ferroelectric nature of the multilayer using an interdigital electrode (IDE) configuration with the application of ±50 V of DC voltage was demonstrated. In the IDE configuration, however, the distribution of the inhomogeneous electric field across the ferroelectric surface leads to low measured permittivity and polarization values of the PZT thin film. Also, information about the ferroelectric-metal electrode interface such as defects and trapped oxygen vacancies that generally exist due to the presence of volatile cationic species such as PbO is obscure in this configuration.[20,21] To overcome the aforementioned issues, a metal electrode based parallel plate capacitor configuration is highly desirable. One may use CVD grown conducting diamond films in order to realize such a configuration. The additional advantage of using a conducting diamond film as a substrate is that this could reduce the fatigue and retention problems in the ferroelectric thin films, which one normally observe when metal electrodes such as Pt and Au are used.[22,23] It is well established that the electrical conductivity of diamond can be tuned by doping of boron. It was found that heavily boron doped diamond films become a superconductor at low

a)Electronic mail: msrrao@iitm.ac.in

temperature (~6 K) with their electrical resistivity at room temperature as low as ~10 mΩ-cm, which can be suitably used as an electrode for diamond based MEMS/NEMS applications and may play an important role in FeRAM devices where PZT is sandwiched between metal and conductive metal oxide electrodes.[24]

We have fabricated a ferroelectric PZT thin film capacitor on a conducting diamond electrode, without any intermediate layers. X-ray diffraction (XRD) and Raman spectroscopy confirmed the pyrochlore free ferroelectric pulsed laser deposition (PLD) grown PZT thin film on the metallic diamond substrate. The aim of this paper is to establish the ferroelectric nature of the PZT/boron doped nanocrystalline diamond (B-NCD) capacitor at the macroscopic and nanoscales and thereby demonstrate the device quality.

The $Pb(Zr_{0.52}Ti_{0.48})O_3$ (PZT) target was synthesized from stoichiometric quantities of the oxide powders PbO, ZrO_2, and TiO_2 by solid state reaction route. 10 mol. % of extra PbO was given during the target preparation, to compensate lead deficiency during sintering and post deposition annealing. A (superconducting) conducting nanocrystalline boron doped diamond (B-NCD) film was grown on a Si substrate using a hot filament chemical vapor deposition (HFCVD) reactor, and the details of the deposition conditions and electrical properties of the films can be found elsewhere.[19,24] The flow rates of CH_4, H_2, and $(CH_3)_3B$ were maintained at 3000, 80, and 40 sccm, respectively. The chamber pressure and the substrate temperature were fixed at 7 Torr and 850 °C, respectively. The B-NCD film was deposited for 2 h resulting in a thickness of 900 nm, and the surface roughness of ~8 nm was observed as estimated from the atomic force microscopy (AFM) measurement (data not shown). The PZT thin films were grown on the B-NCD substrate using the pulsed laser deposition (PLD) technique (Excel Instrument, India). The excimer (KrF) laser with a laser fluence of 2.35 J cm^{-2} was used to ablate the target. The thin film was grown on the substrate at a substrate temperature of 650 °C with 300 mTorr of oxygen partial pressure after evacuating the chamber with a base pressure of 5×10^{-6} mbar. After deposition, the film was subsequently annealed for 30 min at the same temperature, at a pressure of 760 mbar of O_2 partial pressure. After post deposition annealing, the chamber was cooled down to room temperature with a cooling rate of 10 °C per min.

The phase purity and crystalline quality of the films were examined by X-ray diffraction (XRD) analysis (Rigaku X-ray diffractometer equipped with graphite-monochromatic CuK_α radiation (0.15418 nm), operated at 40 kV and 100 mA. Raman spectra of the sample were recorded by using a confocal Raman microscope (Horiba Jobin Yvon), with the exciting line of 488.0 nm of Argon laser. During the measurement, the laser power of 5 mW was maintained with the spot size of 50 μm at the sample. The thickness of the PLD grown PZT thin film on the B-NCD substrate was measured using a field emission scanning electron microscope (FESEM, Quanta 3D). For electrical measurements, Au/Cr top electrodes were coated on the films through a shadow mask by the electron beam evaporation technique and the electrode sizes were 500 μm in diameter. The macroscopic ferroelectric nature of the thin films grown on the B-NCD substrate was shown using a commercial ferroelectric testing system (RT6000S, Radiant Technologies). The nanoscale polarization switching of the sample was recorded using piezo force microscopy (PFM) (Dimension edge, Bruker).

Figure 1(a) shows the XRD result of the PZT thin film grown on the conducting B-NCD substrate. The presence of (001), (110), (111), (002) and (211) peaks in the pattern reflects the formation of a single phase perovskite PZT thin film on the B-NCD substrate. No pyrochlore peak was detected in the scanned range, demonstrating the pyrochlore free ferroelectric phase of the sample. Figure 1(b) depicts the Raman spectra of the PZT/B-NCD multilayer. The Raman peaks originating from the PZT layers are located at 102 cm^{-1} $E(TO_1)$, 140 cm^{-1} $A_1(TO_1)$, 200 cm^{-1} $(E(TO_2)$, 273 cm^{-1} (B_1+E), 326 cm^{-1} $A_1(TO_2)$, 466 cm^{-1} $E(LO_2)$, 535 cm^{-1} $E(TO_3)$, 603 cm^{-1} $A_1(TO_3)$, 702 cm^{-1} $E(LO_3)$, and 750 cm^{-1} $A_1(LO_3)$,[25,26] while Raman signals originating from the B-NCD layers are labelled as pDOS1, pDOS2, ZCP (zone centre phonon), and GBs (grain boundaries). Here, pDOS1 and pDOS2 are the Raman signals due to the violation of the selection rule in the diamond lattice-phonon density of states

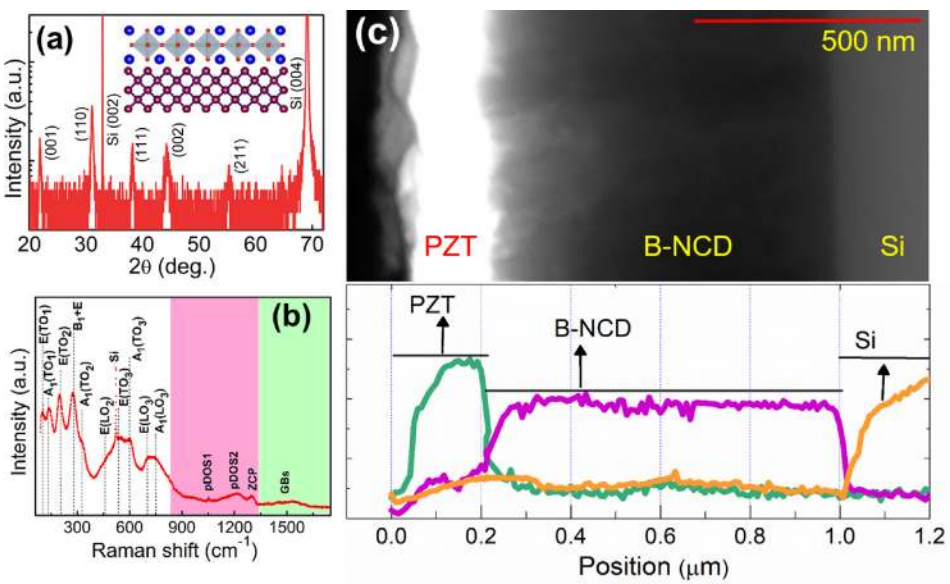

FIG. 1. (a) XRD pattern of the PZT thin film grown on conducting nanocrystalline boron doped diamond (B-NCD) film; the inset depicts the schematic representation of PZT and B-NCD multilayer. (b) Raman spectrum of the PZT/B-NCD multilayer. Various Raman modes originating from the perovskite structure are identified and labelled in the spectrum. The shaded regions indicate the Raman signals originating from the underlying B-NCD film and (c) back scattering cross sectional SEM image with line profiles of the elemental distribution along the cross-section of PZT/B-NCD/Si multilayer.

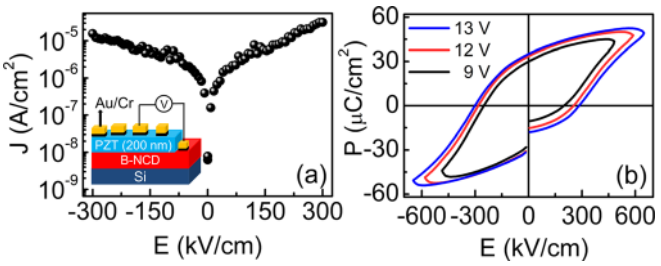

FIG. 2. Leakage current density (J) versus electric field (E) characteristics of the PLD grown PZT thin film on the conducting B-NCD substrate; the inset schematic illustrates the setup used to test the ferroelectric properties of the PZT/B-NCD capacitor. (b) Polarization (P) versus applied electric field (E) hysteresis loops of the sample with different applied voltages.

and GBs are the signals from the grain boundaries of the B-NCD film. The asymmetric peak at 1302 cm^{-1} is the ZCP mode of diamond. This mode is redshifted due to Fano resonance.[24] We can also see a sharp peak at 520 cm^{-1}, which is due to the Si substrate that was used for the diamond growth. Clearly, the PZT thin film grown on top of the B-NCD film is of high quality, and we can further infer from these data that there are no secondary phases formed at the B-NCD/PZT interface. Figure 1(c) shows the back scattering cross sectional SEM image with line profiles of the elemental distribution along the cross-section of the PZT/B-NCD/Si multilayer. From the figure, it has been observed that the interface is clean without any dead layer formation. The line profile of the elemental distribution of the multilayer indicates that there is no inter diffusion of Pb into a heavily boron doped NCD substrate. The thickness of B-NCD is found to be 900 nm, which indicates that the B-NCD layer has not been etched due to oxygen reaction while doing PZT deposition in oxygen ambient. However, we still need to carry out a detailed investigation to further understand the interface properties, which is under investigation.

In order to elucidate the ferroelectric nature of the PLD grown PZT thin film on the B-NCD substrate, the macroscopic polarization switching measurement was performed on the sample. Figure 2(a) depicts the leakage current density (J) as a function of applied electric field (E), and Fig. 2(b) presents the hysteresis (P-E) loops of the sample recorded at various voltages at a constant frequency of 1 kHz. Our result shows a leakage current density of the order of 10^{-5} A/cm^2 for an applied electric field of 300 kV/cm. In the earlier publications, it was shown that asymmetric J-E loops are due to the charge carriers which are present at the interface when the Al_2O_3 film was used as a buffer layer.[15] Note that a symmetrical low leakage current density as observed [shown in Fig. 2(a)] in both quadrants points to the fact that our sample is free from unwanted trapped charge carriers as commonly detected at the interface. This points to the highly insulating behaviour of the sample, which enables the high field polarization studies of the PLD grown sample on the B-NCD substrate.[27] The P-E response [shown in Fig. 2(b)] was measured for different driving voltages of 9, 12 and 13 V, using a measurement frequency of 1 kHz at 300 K. The remanent polarization ($2P_r$) and coercive field of the sample under a maximum applied voltage of 13 V were found to be 68 $\mu C/cm^2$ and 293 kV/cm, respectively. The well saturated and symmetric loops ($+P_r = -P_r$) are a direct consequence of the highly crystalline quality and stoichiometry of the ferroelectric PZT thin film grown on a conducting B-NCD substrate.[10] We have achieved a high value of $2P_r = 68\ \mu C/cm^2$ upon an applied voltage of 13 V. This is the highest polarization value achieved so far when compared with the earlier reports of PZT thin films grown on the diamond substrate.[10,15,19]

From the Raman data and the ferroelectric polarization switching (*i.e.,* P-E loops) measurements, the ferroelectric nature of the PZT thin film grown on the B-NCD substrate on a macroscopic scale is confirmed. To further investigate its ferroelectricity at the nanoscale, we have performed the local polarization switching using the PFM technique. Figures 3(a) and 3(b) present out-of-plane PFM phase and PFM amplitude images of the PZT thin film grown on the conducting B-NCD substrate. The images are $20 \times 20\ \mu m^2$. In order to get a better insight into the ferroelectric polarization switching, an external dc voltage was applied to the bottom electrode, while grounding the conducting tip. Square patterns in the image were poled with $+10\ V_{dc}$ applied to the $10 \times 10\ \mu m^2$ region and $-10\ V_{dc}$ applied to the $5 \times 5\ \mu m^2$ region, and the areas under the bright and dark squares illustrate the change of the polarization state after switching of the as-grown sample, biased at +10 V and −10 V, respectively. Figure 3(c) shows the local polarization switching of PFM amplitude (in red) and PFM phase (in blue) versus bias voltage loop of the sample grown on the B-NCD substrate. The PFM phase hysteresis loop of the sample shows a sharp polarization switching with a phase difference of nearly 180° rather than by 90° rotation, reflecting the presence of ferroelectricity at the nanoscale. A small difference of the

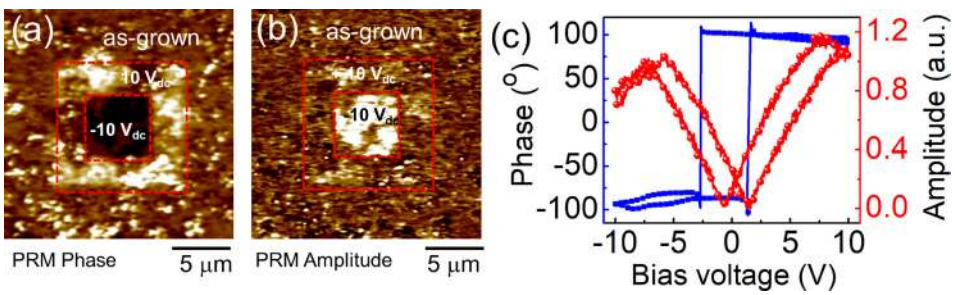

FIG. 3. Out-of-plane (a) PFM phase and (b) PFM amplitude images of the PZT thin film grown on the conducting B-NCD substrate. The images are $20 \times 20\ \mu m^2$. Square patterns were poled with $+10\ V_{dc}$ applied to the $10 \times 10\ \mu m^2$ region and $-10\ V_{dc}$ applied to the $5 \times 5\ \mu m^2$ region; the areas under the bright and dark squares illustrate the change of the polarization state after switching the as-grown sample, biased at +10V and −10 V, respectively, and (c) local switching spectroscopy (in red) PFM amplitude and (in blue) PFM phase versus bias voltage loop of the sample grown on the B-NCD substrate showing clear ferroelectric switching behavior.

coercive voltages ($-V_c$ and $+V_c$) in the hysteresis loop indicates that the interface between the PZT and HFCVD grown B-NCD substrate has low trap charged defects without any dead layers.[11,28–31] The PRM amplitude versus bias voltage shows an excellent butterfly loop with zero voltage offset and a symmetric minima in both the quadrants.

For the device applications, the variation of switchable polarization as functions of the switching cycles, *i.e.,* fatigue measurements of the PZT/B-NCD capacitors, is essential. The objective of this study was to understand the stability of switchable polarization by polarization switching of the ferroelectric thin film capacitor. Figure 4 shows the electrical fatigue measurement, *i.e.,* the suppression of the remanent polarization on repetitive field cycling of the capacitors. The polarization-switching cycle measurement of the sample was carried out with a rectangular pulse width of 5 μs at a repetition frequency of 100 kHz. Our result shows that the remanent polarization did not change until 1×10^7 cycles and thereafter a sudden decrease in the polarization value till 1×10^{10} cycles. It is observed that the fatigue of the thin film capacitors originated after 10^7 switching cycles and decreased to about 10% of the initial value, *i.e.,* of unfatigued state, at the completion of 10^{10} cycles. The symmetry of the hysteresis loop during the measurements along the polarization axis points to, once again, the absence of an internal field between the ferroelectric thin films and the conducting B-NCD substrate.[32,33] This reflects that there is a good adhesion between the PZT thin film and the conducting electrode. After the endurance test (after the completion of the 10^{10} cycles), we recorded the P-E loop of the sample.[34] It indicates that the PZT thin film on the B-NCD electrode is a suitable candidate for various ferroelectric applications such as MEMS/NEMS actuators, radio frequency MEMS, high frequency resonators, and radio frequency (RF) MEMS switches.

We have deposited a ferroelectric PZT thin film using PLD on a HFCVD grown conducting boron doped diamond film without using any intermediate layers. The B-NCD film also served as the bottom electrode, thereby addressing the issue related to fatigue and retention, as generally observed when metal electrodes (Au, Pt, *etc.*) are used. The formation of a single phase perovskite ferroelectric PZT thin film on the B-NCD substrate was confirmed from the XRD pattern and Raman spectroscopy studies. The absence of pyrochlore phases in the PZT/B-NCD multilayer leads to a low symmetrical leakage current density of the order of 10^{-5} A/cm^2 for an applied electric field of 300 kV/cm. Our result showed a well saturated hysteresis loop with a remanent polarization ($2P_r = 68$ μC/cm^2) and coercive field (=293 kV/cm) of the sample under a maximum applied voltage of 13 V. The existence of nanoscale ferroelectric switching of the sample was observed using the switching spectroscopy PFM technique. From the electrical fatigue measurement with 10^{10} switching cycles of the sample, a small degradation of remanent polarization of about 10% was observed, suggesting the high quality of the deposited PZT thin film. The collective experimental results reflect that B-NCD thin films can be used as a bottom electrode for the ferroelectric sample, and therefore, this paves the way for achieving highly efficient ferroelectric based devices.

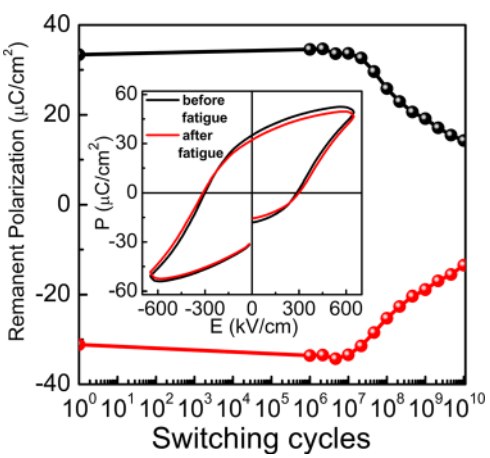

FIG. 4. Remanent polarization as functions of cumulative polarization switching cycles. The inset shows the hysteresis (P-E) loops before and fatigued states after being subjected to 10^{10} switching cycles of the PLD grown PZT thin films on a conducting B-NCD substrate.

This work was supported by the Department of Science and Technology (DST), New Delhi, which facilitated the establishment of "Nano Functional Materials Technology Centre" (Grant No. SRNM/NAT/02-2005) and supported by Defence Research and Development Organization (DRDO), New Delhi (Grant No. PHY/13-14/286/MSRA/DRDO).

[1]A. V. Sumant, O. Auciello, M. Liao, and O. A. Williams, MRS Bull. **39**, 511 (2014).
[2]C. Ko, Y. Lee, Y. Chen, J. Suh, D. Fu, A. Suslu, S. Lee, J. D. Clarkson, H. S. Choe, S. Tongay, R. Ramesh, and J. Wu, Adv. Mater. **28**, 2923 (2016).
[3]J. Rodriguez-Madrid, G. Iriarte, D. Araujo, M. Villar, O. Williams, W. Muller-Sebert, and F. Calle, Mater. Lett. **66**, 339 (2012).
[4]N. Setter, D. Damjanovic, L. Eng, G. Fox, S. Gevorgian, S. Hong, A. Kingon, H. Kohlstedt, N. Y. Park, G. B. Stephenson, I. Stolitchnov, A. K. Taganstev, D. V. Taylor, T. Yamada, and S. Streiffer, J. Appl. Phys. **100**, 051606 (2006).
[5]V. Nagarajan, I. G. Jenkins, S. P. Alpay, H. Li, S. Aggarwal, L. Salamanca-Riba, A. L. Roytburd, and R. Ramesh, J. Appl. Phys. **86**, 595 (1999).
[6]D. Damjanovic, Rep. Prog. Phys. **61**, 1267 (1998).
[7]R. Ramesh, S. Aggarwal, and O. Auciello, Mater. Sci. Eng., R **32**, 191 (2001).
[8]S. Srinivasan, J. Hiller, B. Kabius, and O. Auciello, Appl. Phys. Lett. **90**, 134101 (2007).
[9]R. Ramesh, A. Inam, W. K. Chan, F. Tillerot, B. Wilkens, C. C. Chang, T. Sands, J. M. Tarascon, and V. G. Keramidas, Appl. Phys. Lett. **59**, 3542 (1991).
[10]M. Liao, Y. Gotoh, H. Tsuji, K. Nakajima, M. Imura, and Y. Koide, J. Appl. Phys. **107**, 024101 (2010).
[11]E. A. Paisley, H. S. Craft, M. D. Losego, H. Lu, A. Gruverman, R. Collazo, Z. Sitar, and J.-P. Maria, J. Appl. Phys. **113**, 074107 (2013).
[12]M. Feng, J.-J. Wang, J.-M. Hu, J. Wang, J. Ma, H.-B. Li, Y. Shen, Y.-H. Lin, L.-Q. Chen, and C.-W. Nan, Appl. Phys. Lett. **106**, 072901 (2015).
[13]M. D. Losego and M. Jon-Paul, J. Am. Ceram. Soc. **93**, 3983 (2010).
[14]M. Es-Souni, M. Kuhnke, S. Yakovlev, C.-H. Solterbeck, and A. Piorra, Appl. Phys. Lett. **86**, 022907 (2005).
[15]M. Liao, M. Imura, X. Fang, K. Nakajima, G. Chen, and Y. Koide, Appl. Phys. Lett. **94**, 242901 (2009).
[16]O. Auciello, S. Pacheco, A. V. Sumant, C. Gudeman, S. Sampath, A. Datta, R. W. Carpick, V. P. Adiga, P. Zurcher, Z. Ma, H. c Yuan, J. A. Carlisle, B. Kabius, J. Hiller, and S. Srinivasan, IEEE Microwave Mag. **8**, 61 (2007).
[17]A. V. Sumant, O. Auciello, R. W. Carpick, S. Srinivasan, and J. E. Butler, MRS Bull. **35**, 281 (2010).
[18]C. K. Kwok and S. B. Desu, J. Mater. Res. **8**, 339 (1993).
[19]M. Chandran, B. Tiwari, C. R. Kumaran, S. K. Samji, S. S. Bhattacharya, and M. S. R. Rao, J. Phys. D: Appl. Phys. **45**, 202001 (2012).

[20]H. N. Al-Shareef, D. Dimos, W. L. Warren, and B. A. Tuttle, J. Appl. Phys. **80**, 4573 (1996).
[21]G. E. Pike, W. L. Warren, D. Dimos, B. A. Tuttle, R. Ramesh, J. Lee, V. G. Keramidas, and J. T. Evans, Jr., Appl. Phys. Lett. **66**, 484 (1995).
[22]T. Nakamura, Y. Nakao, A. Kamisawa, and H. Takasu, Appl. Phys. Lett. **65**, 1522 (1994).
[23]N. Takashi, N. Yuichi, K. Akira, and T. Hidemi, Jpn. J. Appl. Phys. **33**, 5207 (1994).
[24]D. Kumar, M. Chandran, and M. S. R. Rao, Appl. Phys. Lett. **110**, 191602 (2017).
[25]E. B. Araujo, K. Yukimitu, J. C. S. Moraes, L. H. Z. Pelaio, and J. A. Eiras, J. Phys.: Condens. Matter **14**, 5195 (2002).
[26]E. Buixaderas, I. Gregora, M. Savinov, J. Hlinka, L. Jin, D. Damjanovic, and B. Malic, Phys. Rev. B **91**, 014104 (2015).
[27]L. Yan, J. Li, H. Cao, and D. Viehland, Appl. Phys. Lett. **89**, 262905 (2006).
[28]I. K. Bdikin, J. A. Perez, I. Coondoo, A. M. R. Senos, P. Q. Mantas, and A. L. Kholkin, J. Appl. Phys. **110**, 052003 (2011).
[29]O. Auciello, J. F. Scott, and R. Ramesh, Phys. Today **51**(7), 22 (1998).
[30]A. M. Bratkovsky and A. P. Levanyuk, Appl. Phys. Lett. **89**, 253108 (2006).
[31]M. B. Okatan and S. P. Alpay, Appl. Phys. Lett. **95**, 092902 (2009).
[32]W. L. Warren, D. Dimos, B. A. Tuttle, R. D. Nasby, and G. E. Pike, Appl. Phys. Lett. **65**, 1018 (1994).
[33]T. Mihara, H. Watanabe, and C. A. P. de Araujo, Jpn. J. Appl. Phys. **33**, 3996 (1994).
[34]J. S. Liu, S. R. Zhang, L. S. Dai, and Y. Yuan, J. Appl. Phys. **97**, 104102 (2005).